Micro-optics for ultra-intense lasers?

doi: 10.1063/5.0038023

Micro-optics for ultra-intense lasers

Cite as: AIP Advances **11**, 035214 (2021); https://doi.org/10.1063/5.0038023
Submitted: 21 November 2020 • Accepted: 12 February 2021 • Published Online: 05 March 2021

H. Habara, Amit D. Lad, R. Nagami, et al.

Micro-optics for ultra-intense lasers

Cite as: AIP Advances 11, 035214 (2021); doi: 10.1063/5.0038023
Submitted: 21 November 2020 • Accepted: 12 February 2021 •
Published Online: 5 March 2021

H. Habara,[1,a)] Amit D. Lad,[2,a)] R. Nagami,[1] Prashant Kumar Singh,[2] Gourab Chatterjee,[2] Amitava Adak,[2] Malay Dalui,[2] J. Jha,[2] P. Brijesh,[2] Y. Mishima,[1] K. Nagai,[3] H. Sakagami,[4] Sheroy Tata,[2] T. Madhu Trivikram,[2] M. Krishnamurthy,[2,5] K. A. Tanaka,[1,6] and G. Ravindra Kumar[2,a)]

AFFILIATIONS

[1] Graduate School of Engineering, Osaka University, Suita, Osaka 565 0871, Japan
[2] Tata Institute of Fundamental Research, 1, Homi Bhabha Road, Mumbai 400 005, India
[3] Institute of Innovative Research, Tokyo Institute of Technology, Suzukake-dai, Midori-ku, Yokohama, Kanagawa 226-8503, Japan
[4] Fundamental Physics Simulation Research Division, National Institute for Fusion Science, Toki 509-5292, Japan
[5] TIFR-Center for Interdisciplinary Sciences, 36/P, Gopanpally Village, Serilingampally Mandal, Ranga Reddy District, Hyderabad 500 046, India
[6] Extreme Light Infrastructure–Nuclear Physics, 30 Reatorului, Magurele–Bucharest 77125, Romania

[a)] **Authors to whom correspondence should be addressed:** habara@eei.eng.osaka-u.ac.jp; amitlad@tifr.res.in; and grk@tifr.res.in

ABSTRACT

Table-top, femtosecond lasers provide the highest light intensities capable of extreme excitation of matter. A key challenge, however, is the efficient coupling of light to matter, a goal addressed by target structuring and laser pulse-shaping. Nanostructured surfaces enhance coupling but require "high contrast" (e.g., for modern ultrahigh intensity lasers, the peak to picosecond pedestal intensity ratio $>10^{12}$) pulses to preserve target integrity. Here, we demonstrate a foam target that can efficiently absorb a common, low contrast 10^5 (in picosecond) laser at an intensity of 5×10^{18} W/cm^2, giving ~20 times enhanced relativistic hot electron flux. In addition, such foam target induced "micro-optic" function is analogous to the miniature plasma-parabolic mirror. The simplicity of the target—basically a structure with voids having a diameter of the order of a light wavelength—and the efficacy of these micro-sized voids under low contrast illumination can boost the scope of high intensity lasers for basic science and for table-top sources of high energy particles and ignition of laser fusion targets.

I. INTRODUCTION

Basic electrodynamics[1] tells us that it is not the applied electromagnetic (EM) field but the local field in the close vicinity of an object or on a surface that controls the light–matter interaction. Recent studies indicate that, apart from the best focusing by an external optic, concentration of light benefits tremendously from the enhancement of electric fields by micro-structures and nano-structures in the target.[2–12] Such structures[3–10] have, therefore, been investigated for enhanced coupling, but they may not survive the precursor (prepulse) illumination before the main femtosecond pulse and need high "peak to baseline" intensity contrast of laser pulses;[13–15] otherwise, preplasma formation may lead to self-focusing as well as several other non-linear processes.[16,17] Furthermore, surface structures may demand sophisticated preparation, and therefore, the effort for optimum coupling of light seems doubly demanding. It would, therefore, be attractive to find a structure that can couple light efficiently without placing special demands on the laser pulse. It would also be wise to use natural focusing of light produced by curvy structures (in the form of light caustics[18]), which may enable simple targets and simple laser pulses to achieve intensity enhancement at a lower cost and complexity.

The porous structure of foams offers a much larger surface area for interaction and lower average plasma density than that in a bulk solid. A basic study for fast ignition of inertial fusion[19–21] has shown large increases in the x-ray yield with a low density gold foam with a pore diameter of 300 nm.[22] Very recently, a nanowire array has been used to demonstrate high energy densities.[11] It is important to note that a nano-structured target can be characterized by not only its density but also the size of the structure.[23] In simple

terms, Mie's field enhancement model tells us that energy coupling efficiency becomes largest when the pore size is comparable to the laser wavelength.[24] Both these examples[23,24] show a large difference in the fast electron energy spectra depending on the characteristic structure size. However, all these studies[11,23,24] use ultrahigh contrast pulses (~10^{11}). Here, we design a target for optimum coupling at normal contrast (10^5) and experimentally demonstrate parameters for efficient production of fast electrons. We conceptualize these foam targets as "integrated optics" for intense laser light.

II. DETERMINING OPTIMUM PORE SIZE OF FOAM

We begin by presenting two-dimensional particle-in-cell (2D-PIC) simulations[25] that lead us to the optimum pore size in the foam. 2D-PIC simulations were conducted with the 2–1/2 fully electromagnetic PIC code FISCOF2.[25] We consider a target consisting of pre-ionized Cu^{25+} plasma with different pore diameters from 0 μm (plane) to 10 μm on the interaction surface. The density is fixed at $10n_c$, where n_c is the critical density at the laser wavelength of 0.8 μm. This density is less than that in our experiment, but the simulated plasma is still sufficiently overdense to the laser light. *P*-polarized laser pulses with a duration of 25 fs are normally incident on the target and focused to a spot size of 1 μm–10 μm, providing a peak intensity of >10^{18} W/cm^2. The size of the simulation box is 26 × 8 μm^2. The observation line for accelerated electrons is located at x = 3 μm.

Figure 1 presents electromagnetic field strength distribution, 40 fs after the main pulse injection. Figure 1(a) shows the schematic of interaction for 10 μm foam pore diameter. The incident laser focal spot is varied systematically from 1 μm to 10 μm. Figures 1(b)–1(e) indicate that the highest field enhancement is achieved for a laser spot (w_0) of 10 μm. In addition, the focusing of the EM field is observed at the center of foam [Fig. 1(e)]. The EM field at the center of foam is found to enhance 3–7 times compared to that at the edges. Such foam target induced "micro-optic" function is analogous to the miniature plasma-parabolic mirror.[26]

Figure 1(f) indicates field strength at the surface and the total energy of accelerated electrons (referenced to a plane target) as a

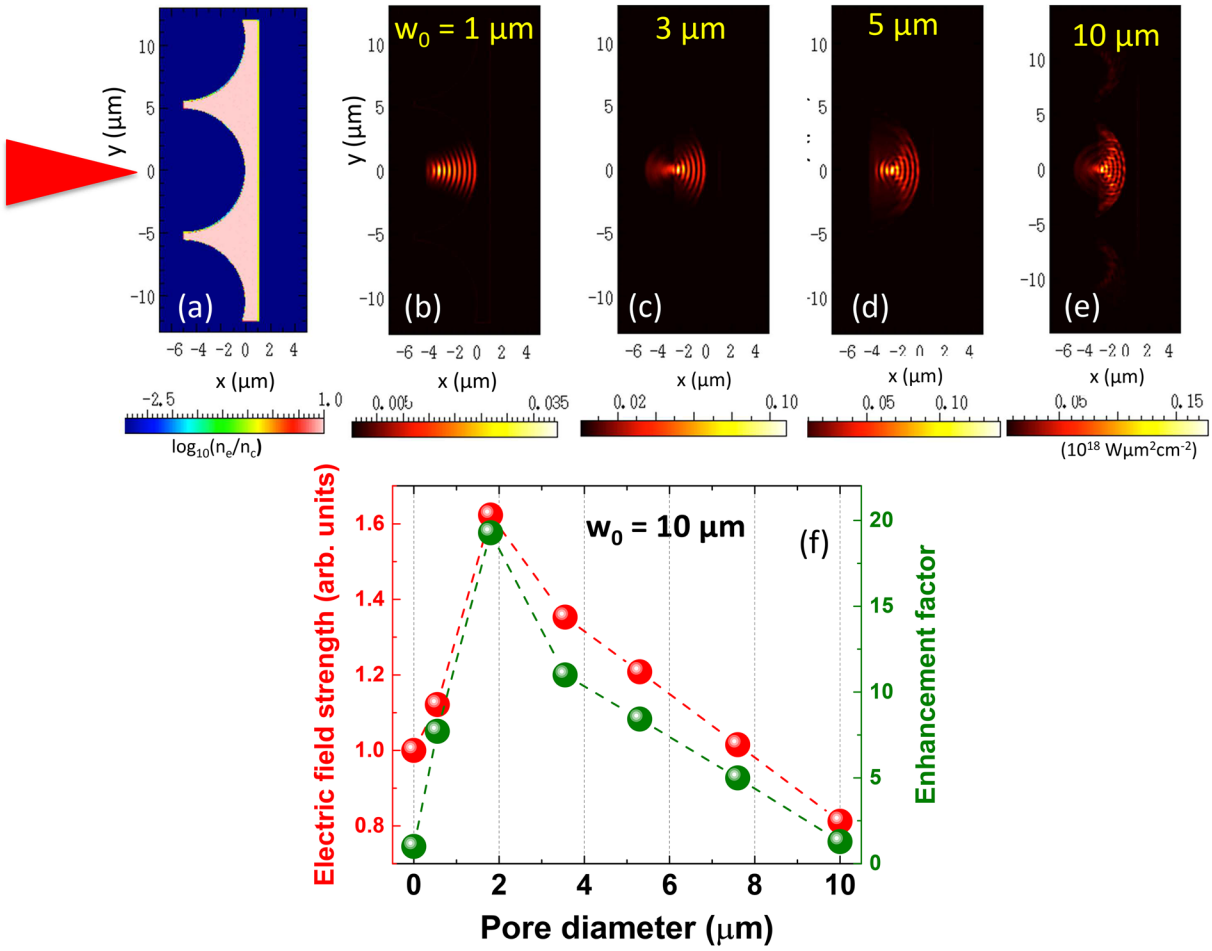

FIG. 1. EM field strength distribution 40 fs after the main pulse injection. (a) Schematic of interaction, with a laser focal spot diameter (w_0) of (b) 1 μm, (c) 3 μm, (d) 5 μm, and (e) 10 μm. (f) EM field strength (red) and enhancement factor of fast electrons (green) as a function of the pore diameter (plain to 10 μm) for a 10 μm laser focal spot.

function of the pore diameter, for a fixed laser focal spot of 10 μm. For 7.6 μm diameter, the field is enhanced five times, but the strength at the surface is lower than that in other cases. This implies that the light concentrated at the center of the pore does not contribute to the electron acceleration. On the other hand, smaller pore diameter limits the laser transmission inside the hole.[27,28] Moreover, the concentrated field energy is smaller as the diameter goes down. Therefore, a pore diameter less than the incident wavelength is less effective than that of larger pores. The electric field enhancement factor indicates that the optimum pore diameter is ~2 μm.

Figures 2(a)–2(c) show electric field intensities, and Figs. 2(e)–2(g) exhibit electron energy density distributions for plane and foam targets detected 40 fs after the incident laser injection. The electric field concentration occurs at the bottom of the pores [Fig. 1(d)] and not at the edges as usually observed, and the concentrated electric field becomes stronger for larger pore diameter and the strength reaches six times the initial value for the 1.9 μm foam. This concentration can be explained by the reflection and refraction of the laser beam at the inner surface of the pore, similar to that of a focusing mirror (see the general discussion later). The larger pore can collect more field energy in its focus, but for a too large diameter, the focus moves away from the inner surface, reducing plasma formation. These conflicting requirements prescribe an optimum pore diameter for efficient laser absorption.

Such enhanced laser field can extract and accelerate a large number of electrons from the target surface. As shown in Fig. 2(g), energetic electrons are pulled out by the laser field propagating along the inner surface. These electrons are accelerated along the laser propagation direction via the $\boldsymbol{J} \times \boldsymbol{B}$ mechanism with enhanced laser fields.[29] Actually, at the rear side of the target [Fig. 2(g)], a bunch of fast electrons are periodically accelerated at twice the laser frequency, consistent with the $\boldsymbol{J} \times \boldsymbol{B}$ mechanism.[29] This highly efficient production of fast electrons can be attributed to the field concentration in the foam followed by collisionless absorption.

A similar calculation for plane foils [Fig. 2(e)] does not show the same level of acceleration as the foams. The efficient laser absorption in foam targets, a possible cause of efficient x-ray emission observed in our previous studies,[22] may result from the lower average density or larger interaction surface than those for a solid plane foil. In other words, the larger foam target adds a geometric factor that enhances fast electron production.

III. EXPERIMENT

We now demonstrate the above predictions by experiments. The experiment is performed with a 20 TW Ti:sapphire chirped pulse-amplified laser at the Tata Institute of Fundamental Research in Mumbai, India, operating at a repetition rate of 10 Hz. The laser has a pulse duration of about 30 fs and a nanosecond prepulse with an intensity contrast (peak to pedestal) of 5×10^6 and 10^5 at 20 ps (inset of Fig. 3). Sharp spikes at ±10 ps and ±20 ps are measurement artifacts. *P*-polarized, 0.8 μm, 30 fs laser pulses irradiate the target at 40° with an $f/3$ off-axis parabolic mirror. The focal spot is about 10 μm diameter corresponding to an intensity of 5×10^{18} W/cm^2. Two magnetic electron spectrometers (ESMs), with image plates as detectors,[30] are installed behind the target along the normal

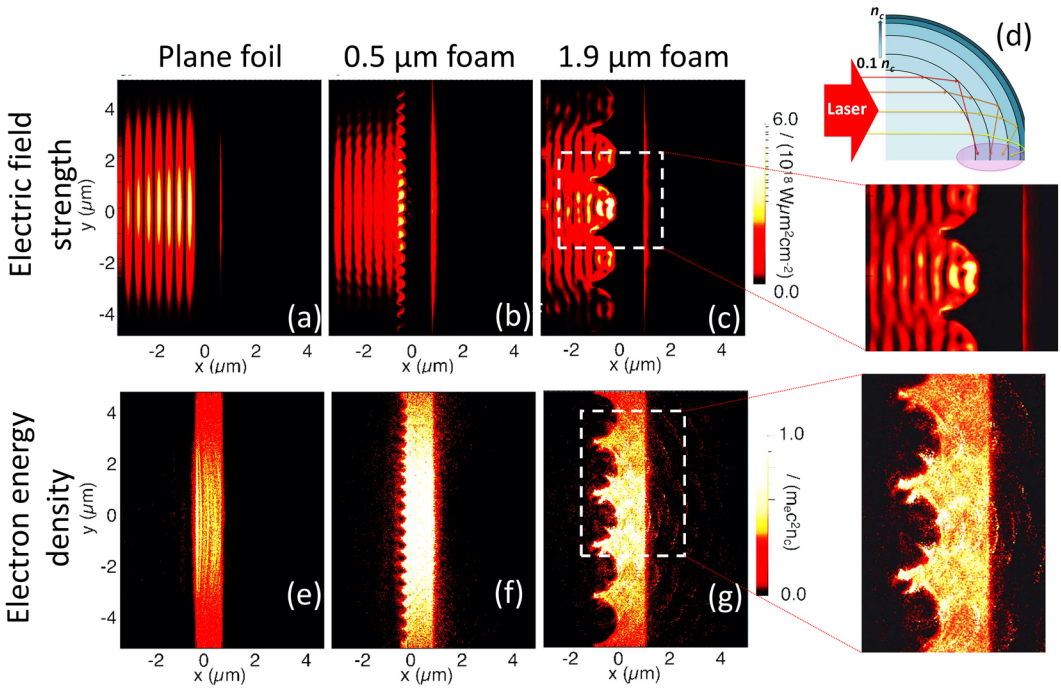

FIG. 2. Electric field strength distribution for (a) a plane Cu foil and (b) 0.5 μm and (c) 1.9 μm of pore diameter foam targets. (d) Schematic of focusing by a pore. Electron energy density distribution for (e) a plane Cu foil and (f) 0.5 μm and (g) 1.9 μm of pore diameter foam targets.

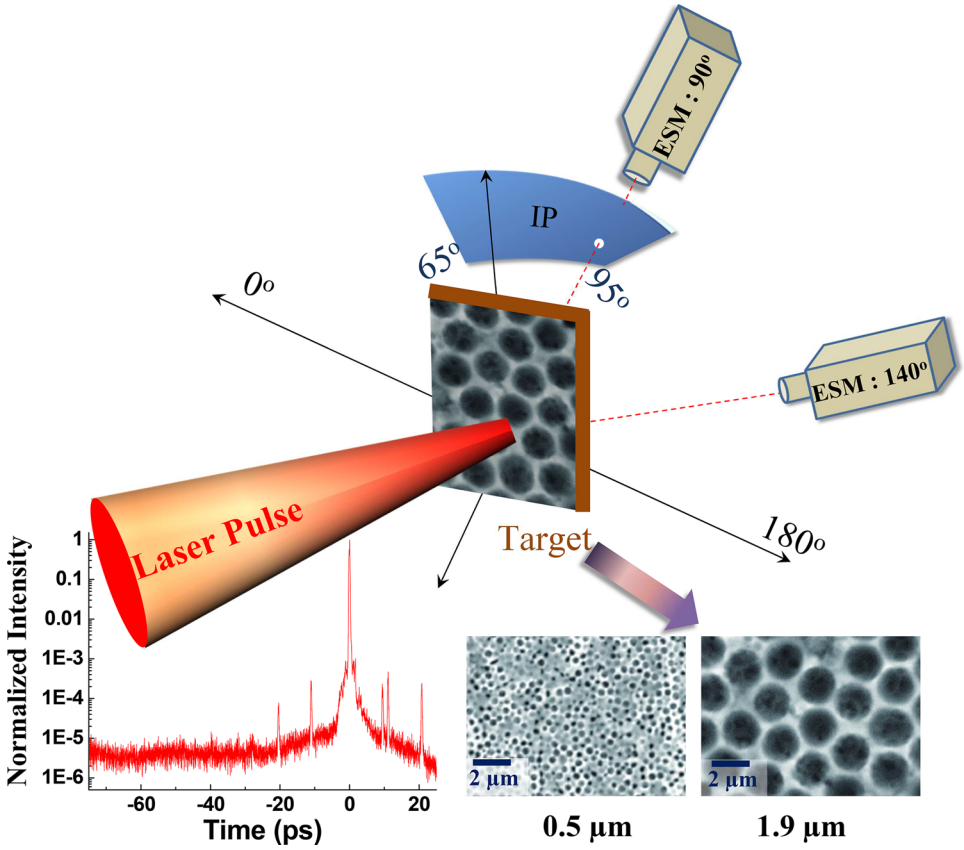

FIG. 3. Experimental setup. A 0.8 μm, *P*-polarized laser pulse irradiates the target at 40°, and accelerated electrons are measured with two ESMs at the target rear: one along the target normal (ESM: 90°) and another along the laser axis (ESM: 140°). An image plate is placed behind the target to measure the angular distribution of the fast electrons exiting the target. Bottom left: Picosecond intensity contrast of the laser pulse. Bottom right: SEM images showing the pore diameter of 0.5 μm and 1.9 μm Cu foam targets. A 2 μm foam layer is coated on a 20 μm copper substrate.

direction (ESM: 90°) and along the laser axis (ESM: 140°). In addition, an image plate is placed a few centimeters behind the target to measure the angular distributions of the fast electrons exiting the target. The image plate has a small hole along the line of sight of the ESM: 90°, to allow for transmission of the electron flux toward the spectrometer.

Our metal nanofoam targets are fabricated by micro-template and electrochemical plating techniques.[31] The electrochemical cell consists of a polystyrene (PS) modified copper electrode ($1 \times 1\ cm^2$) as the working electrode, a copper counter electrode ($2 \times 2\ cm^2$), and a Ag/AgCl reference electrode. We made two types of Cu foam targets, 0.5 μm and 1.9 μm pore diameter with a total foam thickness of 2 μm, deposited on a 20 μm substrate of the copper foil. As PS spheres get accumulated in the hexagonal close-packed system on the back plate, the density of the electrochemical plated foam target is independent of the PS diameter and always 20% that of the solid material. For the same reason, the PS diameter does not change the surface area. As a comparison, a 20 μm polished copper foil is also used in the experiment. Figure 3 also shows scanning electron microscopic (SEM) images of Cu foam targets for 0.5 μm and 1.9 μm pore diameter, respectively. Note the uniformity of pore size and spacing.

IV. RESULTS AND DISCUSSION

Figures 4(a) and 4(b) show the fast electron energy spectra measured along the target normal (90°) and along the laser axis direction (140°), respectively. The fast electron temperature along the target normal (90°) is found to be 49 ± 3 keV for a 20 μm thick plane Cu foil, which increases significantly for foam targets to 132 ± 4 keV (for 0.5 μm pore diameter) and 760 ± 6 keV (for 1.9 μm pore diameter). The fast electron temperature increases ~16 times, whereas the total electron flux increases 11 times for the 1.9 μm foam target compared to the plane foil.

While the electron spectra observed at the laser direction exhibit strong anisotropy, spectra along the laser axis (140°) have ten times less total electrons along with lower electron energy than those along the rear target normal (90°) direction. The fast electron temperature along the laser axis (140°) is found to be 18 ± 2 keV for a Cu foil, which increases significantly for foam targets to

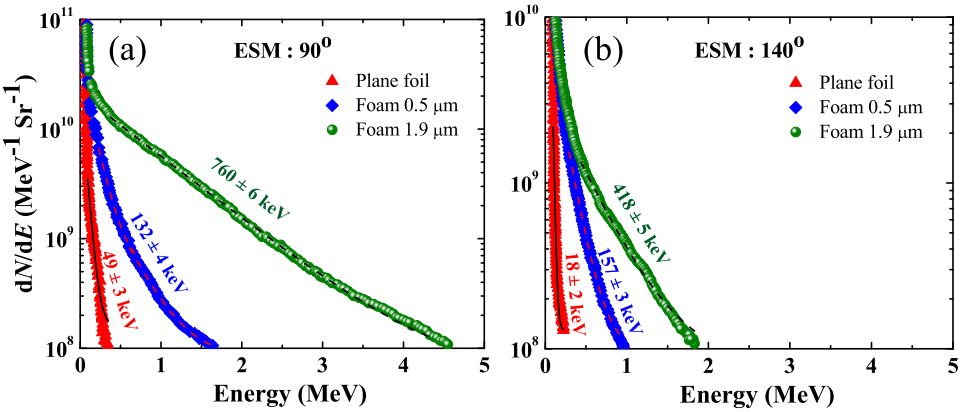

FIG. 4. Electron energy spectra (a) along the target normal (90°) and (b) along the laser axis (140°).

157 ± 3 keV (for 0.5 μm pore diameter) and 418 ± 5 keV (for 1.9 μm pore diameter). The fast electrons are predominantly created for the 1.9 μm foam target, and the total energy is enhanced ~22 times compared to the plane foil. The total electron flux also enhances 11 times for the 1.9 μm foam target compared to the plane foil.

Figures 5(a)–5(c) exhibit the electron angular distributions (IP) of the fast electrons existing the target with the help of IP for a plane foil and 0.5 μm and 1.9 μm diameter Cu foam targets, respectively. Figure 5(d) indicates the line profiles of electron emission captured on an imaging plate located behind the target. It is clear that the electron flux is also significantly enhanced for the 1.9 μm foam target. Note that the signal intensities obtained from the foil and 0.5 μm foam targets are scaled up by a factor of three to facilitate presentation on the same graph. The black lines (Gaussian fit) indicate that the beam divergences are comparable among these targets (~55° in FWHM), in contrast to the near isotropic emission observed in previous studies.[24] We now address the survival of the porous foam structure by the rising edge of the intense laser pulse. Our observations clearly establish the role of the foam structures in the fast electron generation, and so the structures *do play* a role in the interaction at the peak intensity. We argue that a small scale plasma along the porous inner surface, in fact, assists the concentration of the electric field close to that surface, via refraction of the incident light. In fact, our two-dimensional radiative magneto-hydrodynamic (MHD) FLASH simulations[32,33] (carried out using a measured picosecond contrast) clearly indicate that the critical density surface is located very close to the initial inner porous surface (details are in the supplementary material, Sec. S1), although some amount of dilute plasma is created inside the pore. It is interesting to note that the diameter of the pore is also important from the point of view of intensity contrast—the pore should be large enough not to fill up with preplasma before the main femtosecond pulse arrives! All in all, it is very clear that our target design facilitates efficient coupling with no special demands on the laser

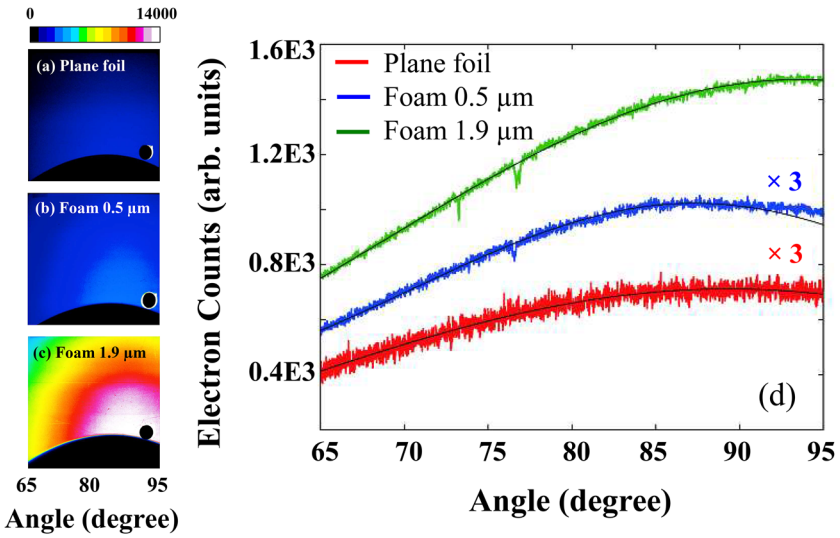

FIG. 5. Electron angular (65°–95°) distribution of the fast electrons exiting the target measured with the help of IP for (a) a plane foil and (b) 0.5 μm and (c) 1.9 μm diameter Cu foam targets. (d) Line profile of electron energy angular distribution, for a plane foil and 0.5 μm and 1.9 μm diameter foam targets.

pulse. We have also measured the self-generated magnetic fields created during intense pulse–foam interactions (details are in the supplementary material, Sec. S2), which further affirms the enhancement of surface field strength of the foam compared to plane foil targets.

We seek to offer some thoughts that may aid generalization of the creation of high light intensities. Can we use the natural focusing of light to enhance the interaction? As is well known from the theory of "caustics"[18] and that of the rainbow,[34] the concentration of light produced by natural structures is omnipresent and much more robust than the focal spot produced by an artificial lens. Structures of all sizes can produce such geometric focusing, but the effects are enhanced when the size becomes comparable to the wavelength. It is perhaps interesting to seek connections with these ideas so that we can further improve the design of targets for intense laser studies.

V. CONCLUSIONS

In summary, porous foam targets demonstrate a great improvement over common, plane targets in coupling normal, low contrast laser pulses even at high, relativistic intensities. The enhanced laser field in the pores effectively accelerates electrons inside the target. This "micro-optic" function of the foam target is quite similar to the small plasma-parabolic mirror, which shows enhancement of energetic ion production.[26] However, we do not need such an expensive small parabolic mirror and an additional target for electron/proton production. Moreover, precise alignment of the focusing optic is not necessary—our target does all these by itself.

SUPPLEMENTARY MATERIAL

See the supplementary material for (S1) estimation of preplasma using 2D radiative MHD simulations and (S2) measurement of self-generated magnetic fields.

AUTHORS' CONTRIBUTIONS

H.H., R.N., and K.A.T. proposed the experiment and conceptualized the execution with G.R.K. R.N., H.H., and K.N. prepared the targets and performed the experiment in collaboration with A.D.L., P.K.S., G.C., A.A., Y.M., T.M.T., S.T., J.J., M.D., P B., and M.K. R.N., A.D.L., H.H., and P.K.S. mainly analyzed the data. R.N. and H.H. performed the computer simulations. All the authors discussed the results and arrived at the conclusions. H.H., A.D.L., G.R.K., P.K.S., and K.A.T. wrote the paper and finalized it with contributions from other authors.

ACKNOWLEDGMENTS

A part of this work was supported by the Grants-in-Aid for Scientific Research, type C (Grant No. 18K03577) and type S (Grant No. 15H05751), the NSFC (Grant Nos. 11991074 and 11721091), and the Science Challenge Project (Grant No. TZ2018005). This work was partially performed under the Cooperative Research Program of Network Joint Research Center for Materials and Devices (Grant No. 20191207) and the Nanotechnology Platform Project (Nanotechnology Open Facilities in Osaka University) of Ministry of Education, Culture, Sports, Science and Technology, Japan (Grant No. F-19-OS-0017). This work was also supported by the "JSPS Asian Core Research and Education Programme, ASHULA." G.R.K. acknowledges partial support from the J. C. Bose Fellowship under Grant No. JCB-037/2010 from the Science and Engineering Research Board, Government of India. The authors also acknowledge the help from T. Matsumoto in the experiments.

DATA AVAILABILITY

The data that support the findings of this study are available within this article and its supplementary material.

REFERENCES

[1] J. D. Jackson, *Classical Electrodynamics* (Wiley, New York, NY, 1999).
[2] T. Nishikawa, H. Nakano, N. Uesugi, M. Nakao, and H. Masuda, "Greatly enhanced soft x-ray generation from femtosecond-laser-produced plasma by using a nanohole-alumina target," Appl. Phys. Lett. **75**, 4079–4081 (1999).
[3] P. P. Rajeev, P. Taneja, P. Ayyub, A. S. Sandhu, and G. R. Kumar, "Metal nanoplasmas as bright sources of hard x-ray pulses," Phys. Rev. Lett. **90**, 115002 (2003).
[4] T. Nishikawa, S. Suzuki, Y. Watanabe, O. Zhou, and H. Nakano, "Efficient water-window x-ray pulse generation from femtosecond-laser-produced plasma by using a carbon nanotube target," Appl. Phys. B **78**, 885–890 (2004).
[5] S. Bagchi *et al.*, "Hot ion generation from nanostructured surfaces under intense femtosecond laser irradiation," Appl. Phys. Lett. **90**, 141502 (2007).
[6] Z. Zhao *et al.*, "Acceleration and guiding of fast electrons by a nanobrush target," Phys. Plasmas **17**, 123108 (2010).
[7] G. Chatterjee *et al.*, "Macroscopic transport of mega-ampere electron currents in aligned carbon-nanotube arrays," Phys. Rev. Lett. **108**, 235005 (2012).
[8] T. Ditmire *et al.*, "High-energy ions produced in explosions of superheated atomic clusters," Nature **386**, 54–56 (1997).
[9] D. Margarone *et al.*, "Laser-driven proton acceleration enhancement by nanostructured foils," Phys. Rev. Lett. **109**, 234801 (2012).
[10] R. Rajeev, T. Madhu Trivikram, K. P. M. Rishad, V. Narayanan, E. Krishnakumar, and M. Krishnamurthy, "A compact laser-driven plasma accelerator for megaelectronvolt-energy neutral atoms," Nat. Phys. **9**, 185–190 (2013).
[11] M. Purvis *et al.*, "Relativistic plasma nanophotonics for ultrahigh energy density physics," Nat. Photonics **7**, 796 (2013).
[12] L. M. Chen *et al.*, "Study of x-ray emission enhancement via a high-contrast femtosecond laser interacting with a solid foil," Phys. Rev. Lett. **100**, 045004 (2008).
[13] J. Itatani, J. Faure, M. Nantel, G. Mourou, and S. Watanabe, "Suppression of the amplified spontaneous emission in chirped pulse-amplification lasers by clean high-energy seed-pulse injection," Opt. Commun. **148**, 70–74 (1998).
[14] N. Minkovski, G. I. Petrov, S. M. Saltiel, O. Albert, and J. Etchepare, "Nonlinear polarization rotation and orthogonal polarization generation experienced in a single-beam configuration," J. Opt. Soc. Am. B **21**, 1659–1664 (2004).
[15] C. Taur, F. Quere, J.-P. Geindre, A. Levy, T. Ceccotti, P. Monot, M. Bougeard, F. Reau, P. D'oliveira, P. Audebert *et al.*, "Plasma mirrors for ultrahigh-intensity optics," Nat. Phys. **3**, 424–429 (2007).
[16] P. Gibbon, *Short Pulse Laser Interactions With Matter* (Imperial College Press, 2005).
[17] Y. Sentoku, V. Y. Bychenkov, K. Flippo, A. Maksimchuk, K. Mima, G. Mouro, Z. M. Sheng, and D. Umstadter, "High-energy ion generation in interaction of short laser pulse with high-density plasma," Appl. Phys. B **74**, 207–215 (2002).
[18] J. F. Nye, *Natural Focusing and Fine Structure of Light: Caustics and Wave Dislocations* (CRC Press, 1999).
[19] M. Tabak *et al.*, "Ignition and high gain with ultrapowerful lasers," Phys. Plasmas **1**, 1626–1634 (1994).
[20] R. Kodama *et al.*, "Fast heating of ultrahigh-density plasma as a step towards laser fusion ignition," Nature **412**, 798–802 (2001).

[21] R. Kodama *et al.*, "Nuclear fusion: Fast heating scalable to laser fusion ignition," Nature **418**, 933–934 (2002).
[22] A. L. Lei *et al.*, "Optimum hot electron production with low-density foams for laser fusion by fast ignition," Phys. Rev. Lett. **96**, 255006 (2006).
[23] L. Cao, Y. Gu, Z. Zhao, L. Cao, W. Huang, W. Zhou, X. T. He, W. Yu, and M. Y. Yu, "Enhanced absorption of intense short-pulse laser light by subwavelength nanolayered target," Phys. Plasmas **17**, 043103 (2010).
[24] O. Klimo, J. Psikal, J. Limpouch, J. Proska, F. Novotny, T. Ceccotti, V. Floquet, and S. Kawata, "Short pulse laser interaction with micro-structured targets: Simulations of laser absorption and ion acceleration," New J. Phys. **13**, 053028 (2011).
[25] H. Sakagami *et al.*, in *Proceedings.of the International Conference on Inertial Fusion Science and Applications, Kyoto, 2001* (Elservier, 2002), pp. 380–383.
[26] M. Nakatsutsumi, A. Kon, S. Buffechoux, P. Audebert, J. Fuchs, and R. Kodama, "Fast focusing of short-pulse lasers by innovative plasma optics toward extreme intensity," Opt. Lett. **35**, 2314–2316 (2010).
[27] T. W. Ebbessen, H. J. Lezec, H. F. Ghaemi, T. Thio, and P. A. Wolff, "Extraordinary optical transmission through sub-wavelength hole arrays," Nature **391**, 667–669 (1998).
[28] C. Genet and T. W. Ebbesen, "Light in tiny holes," Nature **445**, 39–46 (2007).
[29] S. C. Wilks, W. L. Kruer, M. Tabak, and A. B. Langdon, "Absorption of ultra-intense laser pulses," Phys. Rev. Lett. **69**, 1383 (1992).
[30] K. A. Tanaka, T. Yabuuchi, T. Sato, R. Kodama, Y. Kitagawa, T. Takahashi, T. Ikeda, Y. Honda, and S. Okuda, "Calibration of imaging plate for high energy electron spectrometer," Rev. Sci. Instrum. **76**, 013507 (2005).
[31] K. Nagai, D. Wada, M. Nakai, and T. Norimatsu, "Electrochemical fabrication of low density metal foam with mono-dispersed-sized micro- and submicro-meter pore," Fusion Sci. Technol. **49**, 686–690 (2006).
[32] A. Dubey, K. Antypas, M. K. Ganapathy, L. B. Reid, K. Riley, D. Sheeler, A. Siegel, and K. Weide, "Extensible component-based architecture for FLASH, a massively parallel, multiphysics simulation code," Parallel Comput. **35**(10-11), 512–522 (2009).
[33] P. Tzeferacos, M. Fatenejad, N. Flocke, C. Graziani, G. Gregori, D. Q. Lamb, D. Lee, J. Meinecke, A. Scopatz, and K. Weide, "FLASH MHD simulations of experiments that study shock generated magnetic fields," High Energy Density Phys. **17**, 24–31 (2015).
[34] H. M. Nussenzweig, "The theory of the rainbow," Sci. Am. **236**, 116 (1977).